Mechanism of Iberiotoxin Block of the Large-Conductance Calcium-Activated Potassium Channel from Bovine Aortic Smooth Muscle

Kathleen M. Giangiacomo, Maria L. Garcia, and Owen B. McManus*

Department of Membrane Biochemistry and Biophysics, Merck Institute for Therapeutic Research, P.O. Box 2000, Rahway, New Jersey 07065

Received February 6, 1992; Revised Manuscript Received May 1, 1992

ABSTRACT: The interaction of iberiotoxin (IbTX) with the large-conductance calcium-activated potassium (maxi-K) channel was examined by measuring single-channel currents from maxi-K channels incorporated into planar lipid bilayers. Addition of nanomolar concentrations of IbTX to the external side of the channel produced long nonconducting silent periods, which were interrupted by periods of normal channel activity. The distributions of durations of blocked and unblocked periods were both described by single exponentials. The mean duration of the unblocked periods decreased in proportion with the external concentration of IbTX, while the mean duration of the blocked periods was not affected. These results suggest that IbTX blocks the maxi-K channel through a simple bimolecular binding reaction where the silent periods represent times when a single toxin molecule is bound to the channel. In symmetric solutions of 150 mM KCl, with a membrane potential of 40 mV, the mean duration of the blocked periods produced by IbTX was 840 s, and the association rate was 1.3×10^6 M^{-1} s^{-1}, yielding an equilibrium dissociation constant of about 1 nM. Raising the internal potassium concentration increased the dissociation rate constant of IbTX in a manner which was well described by a saturable binding function for potassium. External tetraethylammonium ion increased the average duration of the unblocked periods without affecting the blocked periods, suggesting that tetraethylammonium and IbTX compete for the same site near the conductance pathway of the channel. Increasing the external concentration of monovalent cations from 25 to 300 mM with either potassium or sodium decreased the rate of binding of IbTX to the channel by ~24-fold, with little effect on the rate of toxin dissociation. These findings suggest that IbTX blocks the maxi-K channel with high affinity by occluding the external mouth of the pore and that the interaction of IbTX with the maxi-K channel is strongly influenced by electrostatic interactions.

Iberiotoxin (IbTX), a 37 amino acid polypeptide isolated from the venom of the scorpion *Buthus tamulus*, is a potent blocker of the large-conductance, calcium-activated potassium (maxi-K) channel (Galvez et al., 1990). IbTX exhibits 68% sequence identity with charybdotoxin (ChTX) (Miller et al., 1985; Gimenez et al., 1988), another known peptidyl blocker of the maxi-K channel (Figure 1). The most striking features conserved between the amino acid sequences for ChTX and IbTX are the large number of basic residues (six) and the six cysteine residues which form three disulfide bonds (Cys7–Cys28, Cys13–Cys33, and Cys17–Cys35) (Sugg et al., 1990). Recently, aqueous solution ^{1}H NMR analysis of ChTX (Lambert et al., 1990; Bontems et al., 1991a,b) and IbTX (Johnson & Sugg, 1992) revealed that the two toxins exhibit similar spatial arrangements of their amino acids. Both structures are characterized by three antiparallel β strands forming a β sheet on one face of the molecule and one helix forming the opposite face. In addition, the side chains of five of the six conserved basic residues (Arg25, Lys27, Lys31, Lys32, and Lys34) are localized to the β-sheet face of the molecule. The high sequence homology and the similar three-dimensional structures for ChTX and IbTX suggest that these two toxins may exhibit similar mechanisms for block of the maxi-K channel.

Mechanistic studies on ChTX block of the maxi-K channel from skeletal muscle reveal that ChTX blocks potassium ion conduction by binding to and occluding the extracellular mouth of the pore. The approach of ChTX to its site on the channel is facilitated by electrostatic interactions between negatively charged carboxylates located near the external mouth of the channel and the positively charged amino acid residues on ChTX (Anderson et al., 1988, MacKinnon et al., 1989). Dissociation of ChTX from the channel is probably determined by many types of noncovalent interactions. However, MacKinnon and Miller (1988) have shown that the dissociation rate for ChTX is enhanced by depolarizing membrane potentials and by increasing concentrations of potassium ions which enter the pore of the channel from the intracellular side. They proposed that the observed destabilization of ChTX bound to the channel occurs when potassium occupies a binding site in the pore which senses the electric field. Thus, for ChTX, it is evident that electrostatic interactions are important for defining both the collisional and dissociative components of the ChTX–channel interaction. Since six of the seven positively charged residues found in ChTX are conserved in IbTX, we examined whether the interaction of IbTX with the maxi-K channel was also controlled by electrostatic interactions.

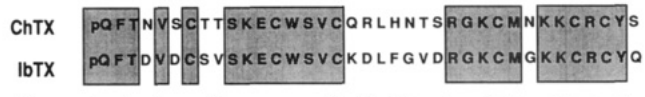

FIGURE 1: Amino acid sequences for iberiotoxin and charybdotoxin. Amino acids conserved between the two toxins are shaded.

In these experiments, we examine the interaction of IbTX with single maxi-K channels from bovine aortic smooth muscle sarcolemmal membranes incorporated into planar lipid bilayers. This method allows us to observe block of a single-channel molecule by toxin under defined experimental conditions. With this approach, we show that IbTX binds to a

* To whom correspondence should be addressed.

0006-2960/92/0431-6719$03.00/0

site in the external mouth of the channel through a simple bimolecular reaction and thereby blocks flux of potassium ions through the channel. Both the collisional and dissociative interactions of IbTX with the maxi-K channel are controlled by electrostatic interactions. An abstract of some of these results has appeared (Giangiacomo et al., 1991).

EXPERIMENTAL PROCEDURES

Materials. Iberiotoxin was purified from venom of the scorpion *Buthus tamulus* as described previously (Galvez et al., 1990). Sarcolemmal membranes were purified from bovine aortic smooth muscle according to previously reported methods (Slaughter et al., 1989). 1-Palmitoyl-2-oleoylphosphatidylethanolamine (POPE) and 1-palmitoyl-2-oleoylphosphatidylcholine (POPC) were purchased from Avanti Lipids, Inc., Birmingham, AL. Bovine serum albumin (BSA), fraction grade V, and ethylene glycol bis(β-aminoethyl ether)-*N*,*N*,*N*',*N*'-tetraacetic acid (EGTA) were purchased from Sigma Chemical Co., St. Louis, MO. 4-(2-Hydroxyethyl)-1-piperazineethanesulfonic acid (HEPES) was from Boehringer Mannheim Biochemical, Indianapolis, IN. Tetraethylammonium chloride (TEA) was from Eastman Kodak Co., Rochester, NY. Sodium chloride was from EM Science, Cherry Hill, NJ. All other salts from Mallinckrodt, Inc., Paris, KY, were >99% pure. Decane from Fisher Scientific, Inc., Springfield, NJ, was 99.9% mole purity.

Fusion of Channels with Planar Lipid Bilayers. Planar lipid bilayers of ~250 pfarad were formed by painting a molar solution of 7:3 POPE/POPC in decane across a 250-μm-diameter hole. Single maxi-K channels were inserted into the lipid bilayer under conditions of an osmotic gradient that promoted fusion of sarcolemmal membrane vesicles with the lipid bilayer. In general, 17 μg/mL membrane vesicles were added to the cis solution (146.3 mM KCl, 5 μM $CaCl_2$, 10 mM HEPES, pH 7.2, and 3.7 mM KOH); the trans solution was 10 mM KCl, 5 μM $CaCl_2$, 10 mM HEPES, pH 7.2, and 3.7 mM KOH. After insertion of a single maxi-K channel into the bilayer, the osmotic gradient was collapsed. The orientation of the channel in the bilayer was determined from the voltage dependence and calcium sensitivity of the channel. Increases in the voltage or calcium concentration at the intracellular face of the channel cause increases in the channel open probability (Barret et al., 1982). Maxi-K channels from our sarcolemmal membrane preparations typically exhibited a 2:1 preference for inserting into the lipid bilayer with the intracellular side exposed to the cis solution. In most experiments, calcium was added to the intracellular side (20–100 μM) so that the channel open probability was >0.7. One millimolar EGTA was added to the solution which bathed the extracellular side of the channel after channel orientation was determined to reduce the possibility of observing additional channels with the opposite orientation. These experimental conditions permitted the study of a single maxi-K channel for up to ~40 h.

All experiments were done at pH 7.20, buffered with 10 mM HEPES and 3.7 mM KOH. The external solution in all experiments contained 15–60 μg/mL BSA and 5 μM $CaCl_2$. The temperature was 22–24 °C.

Single-Channel Data Collection and Analysis. Single-channel currents were measured with a Dagan 3900 voltage clamp (Dagan Corp.) in the mixed RC mode. A 10-kΩ resistor was placed in series with the virtual ground input, and the command voltage was applied to the other side of the bilayer. The amplifier was stable, and the frequency response (>20 kHz) was unaffected by bilayer capacitances of up to 300 pF. The inputs to the amplifier were connected to silver-silver chloride wires immersed in two small wells filled with 0.2 M KCl. Each well was connected to one side of the bilayer with agar bridges containing 0.2 M KCl. The voltage and current are given in the normal electrophysiological convention with the extracellular side of the channel defined as 0 mV and currents flowing from inside to outside plotted in the positive direction.

The currents were filtered at 0.5–2 kHz with a four-pole Bessel filter and digitally encoded onto a video cassette tape with a VR-10 digital data recorder (Instrutech Corp., Elmont, NY). For analysis of open and closed times, the currents were additionally low-pass filtered at 0.3–1 kHz with an eight-pole Bessel filter (Ithaco Model 4302, pulse mode) and played into a DEC 11-73 computer (Digital Equipment Corp.). The filtering was set so that no noise peaks exceeded the 50% threshold level for detecting channel openings and closings. Effective filtering, expressed as dead time, was typically 100–300 μs. The currents were then digitized at no less than five sample points per dead time. The distributions of open and closed times were plotted and fitted with sums of exponential components as previously described (McManus et al., 1987).

The closed times due to toxin block were distinguished from closed times due to normal channel gating by defining a minimum cutoff time for toxin block. For each experiment, the cutoff time, determined from a 30–60-min control period, was assigned a value which either exceeded the longest closed time observed in control or which was 5-fold slower than the slowest time constant seen in the distribution of control closed times. Typically, we used a value of 1–2 s as the cutoff time, which was much longer than the mean closed times of 1–5 ms seen in control and much briefer than the typical mean toxin-blocked times of >500 s. Small changes in the cutoff time had little effect on the results. Unblocked times included all open and closed times separated by toxin blocking events. In some cases, it was faster to measure the blocked and unblocked times directly from the single-channel record. The time constants of the distributions of blocked and unblocked times were determined from maximum likelihood fits with an exponential function or, equivalently, from the mean duration minus the cutoff time. The distributions contained 20–150 events; the expected standard deviations of the time constants of these distributions due to the stochastic nature of the data range from 22 to 8%.

The figures in this paper contain data from over 600 h of analyzed channel data.

RESULTS

IbTX Blocks the Maxi-K Channel from the External Side. IbTX blocks currents flowing through the maxi-K channel with high affinity only when applied to the extracellular side of the channel. Figure 2 shows recordings from a single maxi-K channel which in the absence of toxin was open most of the time. The rapid opening and closing transitions associated with channel gating occur on the millisecond time scale and are not fully resolvable on the slow time scale shown in the figure. Addition of 50 nM IbTX to the intracellular side had no noticeable effect on channel open probability. Subsequent addition of 10 nM IbTX to the extracellular side caused the appearance of long, nonconducting silent periods which were interrupted by periods of apparently normal channel activity. The average duration of the silent periods in this experiment was 18 min, which was thousands of times longer than the mean closed time seen in the control. This effect could be

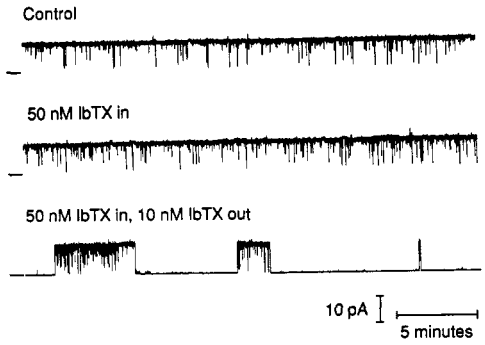

FIGURE 2: IbTX blocks the maxi-K channel from the outside. Currents through a single maxi-K channel are shown in control, after the addition of 50 nM IbTX to the intracellular solution, and then after the addition of 10 nM IbTX to the extracellular solution. The closed-channel current is indicated by the line to the left of the traces, and the channel is open most of the time in control. Conditions: 150 mM KCl *inside and outside*; 50 μM $CaCl_2$ *inside*; +40 mV.

reversed upon washout of IbTX from the extracellular solution (not shown). The simplest interpretation of these data is that the long silent periods report binding of IbTX to a site on the external face of the channel.

IbTX Does Not Affect the Gating Kinetics of the Maxi-K Channel. Since it is possible that IbTX exerts additional inhibitory effects by altering channel gating, we examined the effects of IbTX on the gating kinetics of single maxi-K channels. Figure 3A shows records of a single maxi-K channel before and after the addition of 10 nM IbTX to the outside. In control, the channel is open most of the time, and the transitions associated with channel gating are not resolved on the compressed time scale. Addition of 10 nM IbTX again caused the appearance of long silent periods. We examined the effects of IbTX on maxi-K channel gating by comparing the durations of open and closed times in the absence and presence of toxin. Figure 3B shows the distributions for the open times observed in the absence (line) and presence (circles) of 10 nM IbTX. The two distributions superimpose, suggesting that the toxin has no effect on channel open times. The distributions of closed times are shown in Figure 3C. The closed-time distribution seen in the presence of toxin (circles) can be completely accounted for by the control distribution (line) and a single-exponential component (dashed line) with a time constant of 1033 s. This additional long closed component corresponds to the long silent periods in part A caused by the addition of IbTX. With the exception of the slow component, the distribution of closed durations seen in the absence of IbTX is almost indistinguishable from that observed in the presence of IbTX. Thus, the periods of apparently normal channel activity observed in the presence of IbTX exhibit gating kinetics which are identical to those observed in the absence of toxin. These results suggest that the only measurable effect of IbTX is to cause long silent periods when ions cannot pass through the channel.

IbTX Blocks the Maxi-K Channel through a Simple Bimolecular Reaction. The data presented above suggest that IbTX reversibly binds to the maxi-K channel to produce long nonconducting silent periods. Scheme I describes a simple bimolecular binding reaction which is consistent with these data, where the bursts of normal channel activity occur when

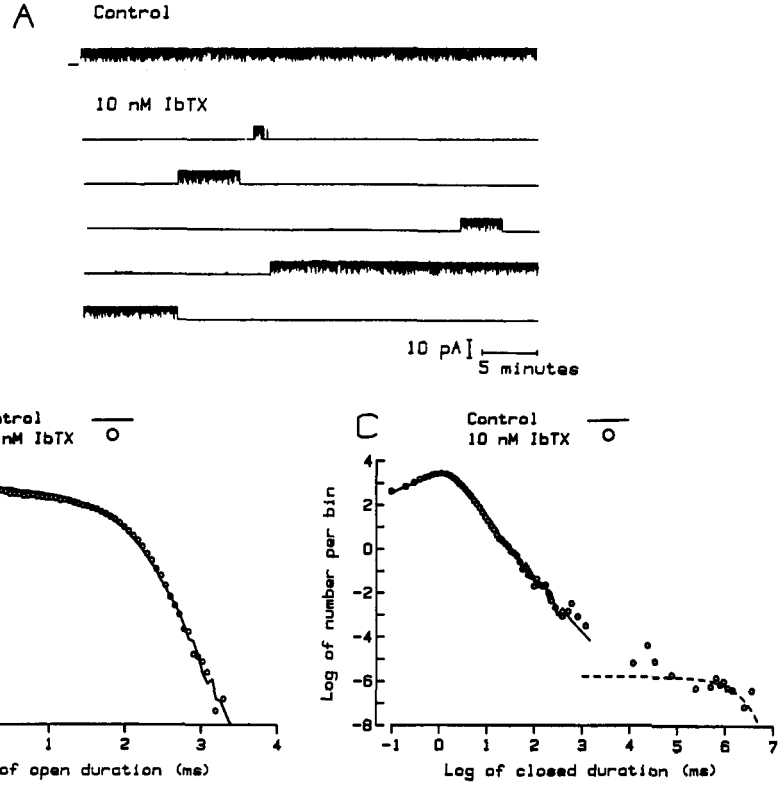

FIGURE 3: IbTX causes long silent periods, but has no other effects on channel gating. (A) Recording from a single maxi-K channel is shown in control and in the presence of 10 nM IbTX on the outside. The closed-channel current level is indicated to the left, and the channel is open most of the time in control. (B and C) Distributions of open (B) and closed (C) times are plotted as the number of events (per 100-μs bin) of a particular duration against their durations. The solid lines plot the distributions of open and closed times observed in control, while the circles plot the distributions observed with 10 nM IbTX outside. The distributions were scaled to contain the same number of events. The dashed line in (C) describes a single-exponential component with a time constant of 1033 s and an area of 0.00015. The distributions of open and closed times observed in the presence of 10 nM IbTX can be entirely accounted for by the control distributions and an additional long-lifetime closed component. The distributions were constructed from 1 h of control data and 4.5 h of data collected in the presence of toxin. Conditions: 300 mM KCl outside; 150 mM KCl and 20 μM $CaCl_2$ inside. The membrane potential was +40 mV.

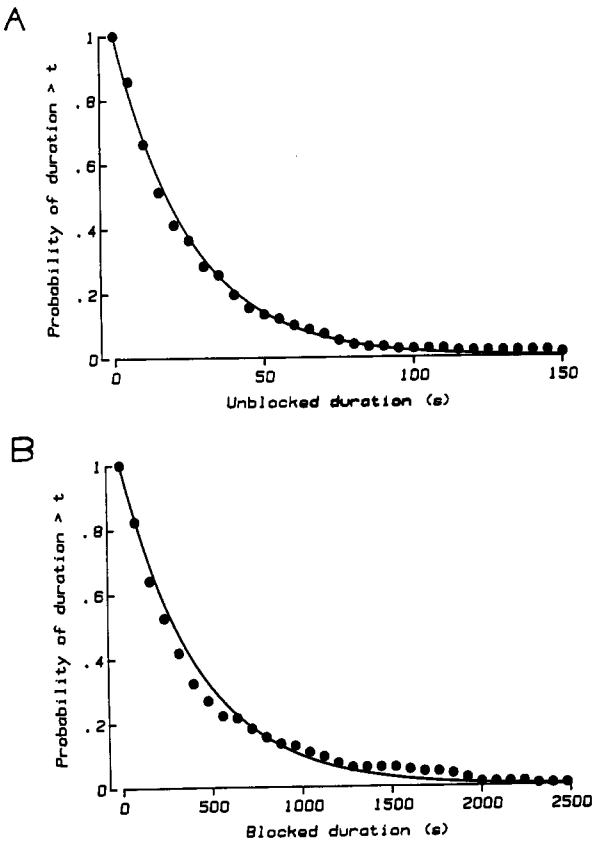

FIGURE 4: Durations of unblocked and blocked times in IbTX are exponentially distributed. The durations of unblocked (A) and blocked (B) events observed in 10 nM IbTX are plotted as cumulative dwell-time distributions. The solid lines plot single-exponential components fit to the data with a time constant of 25.5 s for the unblocked times and 429 s for the blocked times. Distributions were constructed from 148 blocking events and 19 h of continuous recording from a single channel. Conditions: 100 mM KCl outside; 250 mM KCl and 50 μM $CaCl_2$ inside; +40 mV.

toxin is not bound to the channel (C) and the duration of these bursts is related to the pseudo-first-order association rate constant, k_{on}[IbTX]. The long closed times occured when toxin is bound to the channel (C–IbTX), and the duration of these closed times is related to the first-order dissociation rate constant, k_{off}. The equilibrium binding dissociation constant, K_d, is equal to k_{off}/k_{on}. This simple model makes two quantitative predictions. The distributions of blocked and unblocked times should follow single exponentials with the time constant of the blocked durations equal to $1/k_{off}$ and the time constant of the unblocked durations equal to $1/k_{on}$[IbTX], and this model predicts that the time constant for the blocked times will be independent of toxin concentration while the time constant for the unblocked times will decrease in proportion with increases in the concentration of IbTX.

Scheme I

$$C \underset{k_{off}}{\overset{k_{on}[IbTX]}{\rightleftharpoons}} C\text{–IbTX}$$

Figure 4 shows that the distributions of unblocked (part A) and blocked (part B) durations measured in the presence of 10 nM IbTX are both well described by a single-exponential component. Fitting these distributions with sums of two exponential components did not significantly improve the likelihood of the fits. Eight other experiments were analyzed in a similar manner. Of the 18 blocked and unblocked

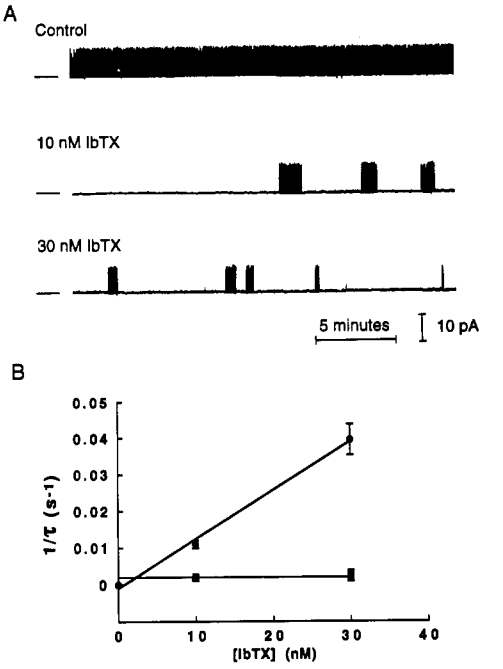

FIGURE 5: Effects of IbTX concentration on blocked and unblocked durations. (A) Recordings from a single maxi-K channel are shown in the absence and presence of 10 and 30 nM external IbTX. (B) Mean values of the reciprocals of the time constants of distributions of the blocked (squares) and unblocked (circles) events are plotted as a function of external IbTX concentration. The line with the unblocked times is the best fit of a straight line to the data, and the line with the blocked times is plotted at the overall reciprocal mean blocked time. Values were determined from five experiments at 10 nM and two experiments at 30 nM with an average of 40 blocking events in each determination. The plotted error bars represent standard errors of the mean. Conditions: symmetric 150 mM KCl and 5–20 μM $CaCl_2$ inside; +40 mV.

distributions, 17 were best fit with a single exponential, while 1 unblocked distribution was best fit with two components. The single observation of a two-component distribution is consistent with the stochastic nature of the data. Therefore, these results are consistent with the predictions of Scheme I.

The effect of IbTX concentration on the blocked and unblocked times is shown in Figure 5. Inspection of the single-channel records in part A reveals that as the IbTX concentration is raised from 10 to 30 nM the blocked durations remain about the same, while the unblocked times decrease. Quantitative analysis of the data from this experiment and four others done under similar conditions is shown in part B. The reciprocal time constants ($1/\tau$) for the blocked times (squares) and the unblocked times (circles) are plotted as a function of the concentration of IbTX. This analysis reveals that the time constants for the blocked times are nearly identical at both toxin concentrations while the reciprocal time constants for the unblocked times increase linearly with toxin concentration. These results exactly match the predictions of the model described in Scheme I where IbTX blocks the channel by binding in a 1 to 1 stoichiometry with pseudo-first-order reaction kinetics.

With this framework, we can use the data in Figure 5 to estimate the rates for toxin binding to and release from the maxi-K channel. The second-order binding rate constant, k_{on}, in Scheme I, determined from the slope of the reciprocal unblocked time constant, was 1.3×10^6 M^{-1} s^{-1}. The dissociation rate constant, k_{off}, estimated from the reciprocals of the mean blocked time constants at both toxin concentrations, was 2.0×10^{-3} s^{-1}. A K_d value of 1.5 nM was calculated from the IbTX concentration at the intersection of the two

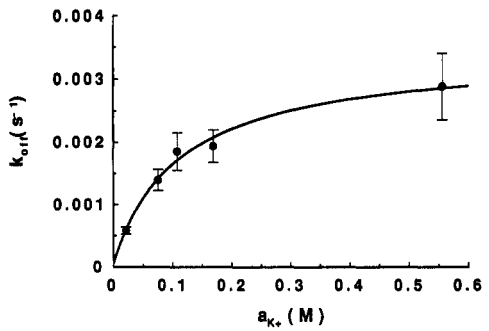

FIGURE 6: Internal potassium enhances the IbTX dissociation rate. Mean k_{off} values and standard errors of the mean are plotted at different internal potassium ion activities with external potassium concentration held constant at 100 mM. The solid line is the best fit to the data with a simple binding equation for potassium (eq 1, see text) using nonlinear χ^2 minimization, with an equilibrium dissociation constant for potassium, K_{K+}, of 110 mM and maximum and minimum dissociation rate constants of 3×10^{-3} and 6×10^{-5} s^{-1}, respectively. The values in this plot were determined from 26 separate experimental measurements with an average of 49 blocking events per measurement, and result from analysis of 320 h of single-channel data. Conditions: 100 mM KCl outside; internal [KCl] was varied from 25 mM to 1 M KCl; +40 mV.

lines in Figure 5B, where the blocking and unblocking rates are equal.

IbTX Blocks the Pore of the Maxi-K Channel. Charybdotoxin binds to a site in the mouth of the maxi-K channel from skeletal muscle and physically occludes the pore (MacKinnon & Miller, 1988). This model was based on the observation that the dissociation rate constant for ChTX was facilitated by increasing the intracellular concentration of permeant monovalent cations such as potassium (MacKinnon & Miller, 1988), an effect referred to as trans-enhanced dissociation. The model was also based on the observation that external tetraethylammonium (TEA), which binds to a site in the mouth of the pore (Villaroel et al., 1988), competes with ChTX for a site on the channel (Miller, 1988). Since IbTX and ChTX share similar structures, we used these two criteria to test whether IbTX also occludes the pore of the maxi-K channel.

Figure 6 shows the average k_{off} values for IbTX determined from several different experiments plotted as a function of the internal potassium ion activity with the external concentration of potassium held constant at 100 mM. The average dissociation rate constant increased by about 7-fold over the concentration range shown, and the effect appears to saturate at high potassium concentrations. The association rate was not affected by the concentration of internal potassium (not shown). These results are consistent with the model for trans-enhanced dissociation (MacKinnon & Miller, 1988) where the occupancy of a single potassium binding site in the conduction pathway of the channel destabilizes the interaction of IbTX with the maxi-K channel. According to this model, when IbTX is bound to the channel (C–IbTX), the potassium binding site is in rapid equilibrium with the internal concentration of potassium. When the potassium site is empty, the interaction of IbTX with the channel is optimal, and the toxin dissociates from the channel with a minimum rate, k_{off}^{min}. When the potassium site is occupied, the interaction of IbTX with the channel (K^+–C–IbTX) is destabilized, and the toxin dissociates from the channel with a maximum rate constant, k_{off}^{max}, as shown by Scheme II. According to this model, the observed dissociation rate constant of IbTX, k_{off}, reports the equilibrium occupancy of the potassium binding site and can

Scheme II

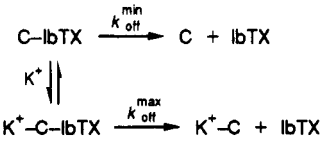

be fit to a simple equilibrium binding equation for potassium described by eq 1,

$$k_{off} = \frac{k_{off}^{max} - k_{off}^{min}}{1 + K_{K+}/a_{K+}} + k_{off}^{min} \quad (1)$$

where K_{K+} is the equilibrium dissociation constant for the potassium site, a_{K+} is the internal potassium ion activity, and k_{off}^{max} and k_{off}^{min} are the dissociation rate constants for IbTX when the potassium binding site is occupied or unoccupied, respectively. The fit to this equation provided a good description of the data shown in Figure 6 with a K_{K+} value for potassium of 110 mM and with k_{off}^{max} and k_{off}^{min} values for IbTX of 3.4×10^{-3} and 6×10^{-5} s^{-1}, respectively. Thus, according to this model, occupancy of the potassium binding site destabilizes the IbTX–channel interaction by 57-fold. The observed trans-enhanced dissociation of IbTX by potassium supports the idea that IbTX blocks by occupying a site near the mouth of the channel.

Externally applied TEA blocks conduction through the maxi-K channel by occupying a site in the pore of the channel near the external mouth (Villaroel et al., 1988). If IbTX and TEA occupy similar or overlapping sites on the channel, then IbTX can bind to the channel only when TEA is not bound, as shown by Scheme III.

Scheme III

$$\text{C–TEA} \underset{\text{TEA}}{\rightleftharpoons} \text{C} \overset{\text{IbTX}}{\rightleftharpoons} \text{C–IbTX}$$

Since the binding and unbinding of TEA are in rapid equilibrium relative to the binding reaction for IbTX, the apparent IbTX association rate with the channel observed in the presence of TEA [$k_{on(TEA)}$] is proportional to the probability that the channel is not occupied by TEA, as shown by eq 2,

$$k_{on(TEA)} = \frac{k_{on}}{1 + [TEA]/K_i} \quad (2)$$

where K_i is the equilibrium inhibitor dissociation constant for TEA and k_{on} is the association rate constant for IbTX in the absence of TEA. The dissociation rate of IbTX should not be affected by the presence of TEA. Similarly, the unitary current amplitude measured in the presence of TEA, I_{TEA}, will be proportional to the probability that the channel is not occupied by TEA:

$$I_{TEA} = \frac{I}{1 + [TEA]/K_i} \quad (3)$$

where I is the unitary current amplitude measured in the absence of TEA. Thus, the model for a competitive interaction between TEA and IbTX predicts that the ratio of the unblocked times for IbTX in the presence and absence of TEA should increase in proportion with the concentration of TEA. The magnitude of this effect should be similar to the magnitude of the apparent current reduction observed in the presence of TEA (Miller, 1988).

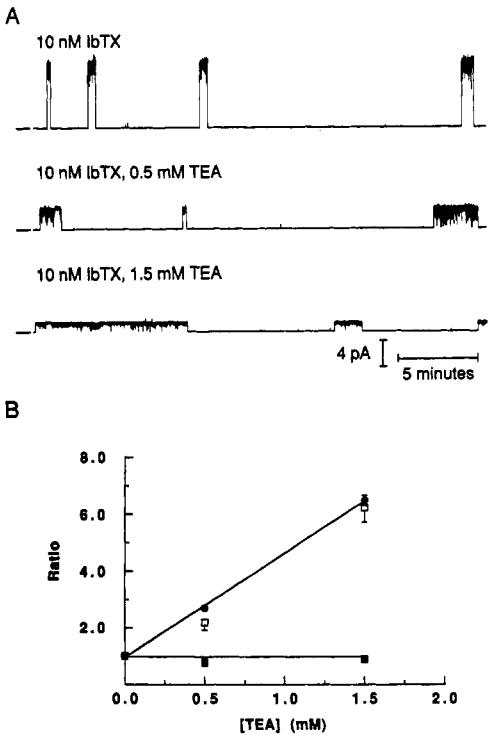

FIGURE 7: External TEA slows the IbTX association rate. Part A shows single-channel records of IbTX block of the maxi-K channel in the absence and presence of 0.5 and 1.5 mM external TEA. Part B plots the ratio of the mean unblocked time in the presence and absence of TEA (filled circles), the ratio of the mean blocked times in the presence and absence of TEA (filled squares), and the ratio of the current in the absence and presence of TEA (open squares) as a function of the concentration of external TEA. The line with the ratio of the unblocked times represents the best fit of the data to a straight line and from the reciprocal of the slope yields a K_i value for TEA of 270 μM. The line plotted with the ratio of the blocked times is plotted at 1. The values plotted at each TEA concentration represent the average values determined from 4 separate experiments with an average of 54 events in each experiment; the plotted errors represent the standard errors of the mean. The values in this plot were determined from analysis of 100 h of single-channel data. Conditions: symmetric 100 mM KCl; +40 mV.

As predicted, the addition of external TEA produces two effects in the single-channel records of IbTX block shown in Figure 7. First, when the channel is not blocked by IbTX, the amplitudes of the unitary currents are significantly reduced relative to currents observed in the absence of TEA. This apparent reduction is due to rapid block of the maxi-K channel by TEA (Blatz & Magleby, 1984; Yellen, 1984). The transitions for TEA block and unblock are so rapid that the individual events cannot be resolved and the current amplitude appears reduced. The other effect of external TEA is a significant increase in the average duration of the unblocked times observed in the presence of IbTX, suggesting that the observed association rate constant, $k_{on(TEA)}$, is slowed by the presence of TEA. The average duration of the blocked times for IbTX did not appear to be altered by externally applied TEA.

These effects of TEA are shown quantitatively in part B of Figure 7. The ratios of the mean unblocked times (filled circles) and mean blocked times (filled squares) in the presence and absence of TEA are plotted as a function of external TEA concentration. The ratios of the current amplitude in the absence of TEA relative to the amplitude in the presence of TEA (open squares) are also plotted as a function of external [TEA]. The data in Figure 7B fulfill the predictions of Scheme III. TEA increased the mean unblocked times for IbTX but had no effect on the mean blocked times. The magnitude of the effect of TEA on the single-channel amplitudes is similar to its effect on the IbTX association rates. A linear fit to the ratio of the mean unblocked times, from the reciprocal slope, yielded a K_i value for TEA of 280 μM. A fit to the ratio of the single-channel current amplitudes yielded a K_i value for TEA of 270 μM.

These results are exactly as predicted for a competitive interaction between TEA and IbTX, where the reduction in the IbTX association rate is proportional to the fraction of time the channel is occupied by TEA (Miller, 1988). Thus, IbTX and TEA behave as strictly competitive inhibitors and must therefore occupy similar or overlapping sites on the channel. Since external TEA occupies a site in the conduction pathway of the channel, these results further support the concept that IbTX binds to a site near the ion conduction pathway of the maxi-K channel.

Effect of External Ionic Strength. IbTX carries a net positive charge which may influence its rate of association with a negative charged binding site on the channel. Our data suggest that IbTX binds near the external mouth of the channel, and previous data have demonstrated that the maxi-K channel from skeletal muscle carries fixed negative charges near the channel mouth which influence ChTX binding (MacKinnon & Miller, 1989; MacKinnon et al., 1989). If electrostatic interactions between negative charges on the channel and positive charges on IbTX promote the observed rate of binding, then screening of these fixed charges at high ionic strength should decrease the observed toxin association rate. We examined the influence of external ionic strength on the rates of IbTX binding to and release from the maxi-K channel in order to investigate the role of fixed charges on the collisional interaction of IbTX with the channel.

Figure 8 shows that the external ionic strength alters the kinetics of IbTX block of the maxi-K channel. As the external KCl concentration is increased from 25 to 300 mM, the toxin association rate decreased by about 24-fold (part A). In contrast, the same changes in the external potassium concentration had no effect on the toxin dissociation rate (part B). The data in Figure 8A are well described by the Bronsted–Bjerrum equation (eq 4).

$$k_{on} = k_{on}^{0} e^{2\alpha Z_c Z_t \sqrt{I_S}} \quad (4)$$

This approach uses Debye–Huckel theory (Bronsted, 1922; Wherland & Gray, 1976) to predict the relationship between the ionic strength, I_S, and the observed collisional rate constant, h_{on}, where k_{on}^{0} represents the collisional rate constant at zero ionic strength, Z_c and Z_t represent the net charge on the channel binding site and on the toxin binding site, respectively, and α has a constant value of 1.17 at 23 °C. The best fit of the data to eq 4 yielded a k_{on}^{0} value of 5.3×10^7 M^{-1} s^{-1} and a Z_cZ_t value of −3.7. The Z_cZ_t value obtained from the fit may not accurately predict the net charge product on IbTX and the channel since this model assumes that IbTX and the channel behave as oppositely charged spheres. However, the agreement between theory and data suggests that, at the ionic strengths tested, IbTX and the channel mouth behave as oppositely charged molecules which are screened by nonspecific ionic interactions. This is further supported by the observation that qualitatively similar effects were observed with sodium.

DISCUSSION

IbTX Blocks the Maxi-K Channel by a Simple Mechanism. In this study, we have investigated the mechanism for IbTX block of the large-conductance calcium-activated

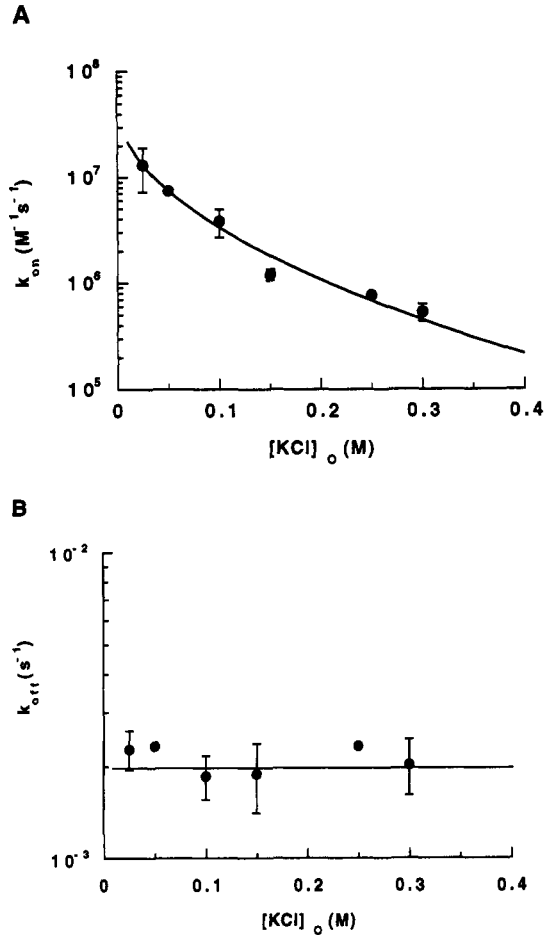

FIGURE 8: Effect of external potassium concentration on the blocking kinetics of IbTX. The second-order association rate constant for IbTX (A) and the dissociation rate constant for IbTX (B) are plotted as a function of the external concentration of KCl. The line in (A) describes the best fit to the data with the Bronsted–Bjerrum equation (eq 4) with a charge product for IbTX and the channel of –3.7. The line in (B) represents the overall mean dissociation rate constant. The values in this plot were determined from 22 separate experimental measurements with an average of 45 blocking events per measurement, and result from analysis of 180 h of single-channel data. The error bars represent the standard errors of the means. Conditions: the internal KCl concentration was 150 mM; +40 mV.

potassium channel in bovine aortic smooth muscle. Our experimental data were well described by a model in which IbTX reversibly binds to a site near the external mouth of the channel and thereby blocks the movement of ions through the channel. Binding of IbTX to the channel is manifested in long silent periods lasting about 10 min when no current passes through the channel. These long silent periods are interrupted by periods of normal channel activity that represent times when toxin is apparently not bound to the channel.

A previous report suggested that IbTX altered the gating of maxi-K channels in outside-out patches excised from cultured bovine aortic smooth muscle cells (Galvez et al., 1990). In our experiments with maxi-K channels from bovine aortic smooth muscle inserted into planar lipid bilayers, IbTX caused long silent periods, with no other changes in channel gating. In order to determine whether this discrepancy is due to differences in the experimental conditions, we also examined IbTX block of the channel in bilayers composed of charged phospholipids (PE/PS 1:1), with or without 1–2 mM magnesium on the inside. We were unable to identify any other effects of IbTX, besides the long blocked periods. Candia et al. (1991) similarly found that IbTX caused long silent periods, but had no other effects on gating of maxi-K channels from skeletal muscle.

Location of the IbTX Binding Site. IbTX blocks the maxi-K channel only when added to the outside. Two different sets of experimental observations locate the external binding site for IbTX near the entrance to the pore as shown in Figure 9.

Internal potassium ions enhance the rate of dissociation of IbTX from its binding site on the external side. This effect can be explained by a simple model (MacKinnon & Miller, 1988) where occupancy of a potassium binding site in the pore destabilizes the interaction of IbTX with the channel. When IbTX is bound to the outside of the channel, potassium sites within the pore rapidly equilibrate with the bulk concentration of internal potassium. As the internal potassium concentration is increased, equilibrium occupancy of a potassium site in the pore is also increased. In terms of this model, we found that potassium binds to a site in the pore with an apparent equilibrium dissociation constant of 110 mM and, when the site is fully occupied, increases the rate of IbTX dissociation by 57-fold. A similar effect of internal permeant ions on dissociation of external blockers has been observed in the maxi-K (Yellen, 1984; MacKinnon & Miller, 1988) and other potassium channels (Bezanilla & Armstrong, 1972). These data argue that IbTX binds near the conduction pathway of the maxi-K channel. However, we cannot rigorously exclude other explanations involving conformational changes induced by internal potassium.

The second piece of evidence which locates the IbTX binding site near the pore is that external TEA displays a strictly competitive interaction with IbTX. This suggests that the binding sites for TEA and IbTX overlap. Since external TEA binds to a site in the pore that senses about 20% of the voltage drop across the channel (Yellen, 1984; Villaroel et al., 1988), these findings suggest that IbTX binds to a site very near the entrance to the pore of the maxi-K channel.

Local Charges on the Channel Enhance the IbTX Association Rate. The rate of association of IbTX with the channel decreased as the external ionic strength was increased (Figure 8). This behavior can be explained by proposing that the rate of association of a positively charged IbTX with a negatively charged channel mouth is promoted by electrostatic interactions. Increasing the ionic strength should attenuate the Coulombic attraction and thereby slow the observed association rate. As a first approximation, we have described our data with a model (eq 4) based on Debye–Huckel theory (Bronsted, 1922; Wherland & Gray, 1976) which assumes that IbTX and the channel behave as oppositely charged spheres. This treatment provided a reasonably good fit to the data, yielding a charge product for IbTX and the channel of –3.7, and a k_{on} value at zero ionic strength of 5.3×10^7 M^{-1} s^{-1}.

Other electrostatic models, such as Gouy–Chapman, have been used to model the effects of ionic strength on binding of charged toxins with channels in planar lipid bilayers (Green et al., 1987; MacKinnon et al., 1989). We found that Gouy–Chapman theory poorly predicted the effects of ionic strength on IbTX association rates (not shown). A variation of the Gouy–Chapman model assumes that the toxin competes with a charged ion, such as sodium or potassium, for a binding site on the channel and that the local concentrations of the toxin and the competing ion are described by Gouy–Chapman theory. This model predicted the effects of external sodium ion concentration on tetrodotoxin binding to sodium channels in lipid bilayers (Greene et al., 1987; Ravindran & Moczydlowski, 1989) but did not account for the effects of potassium concentration on IbTX binding in our experiments (not shown).

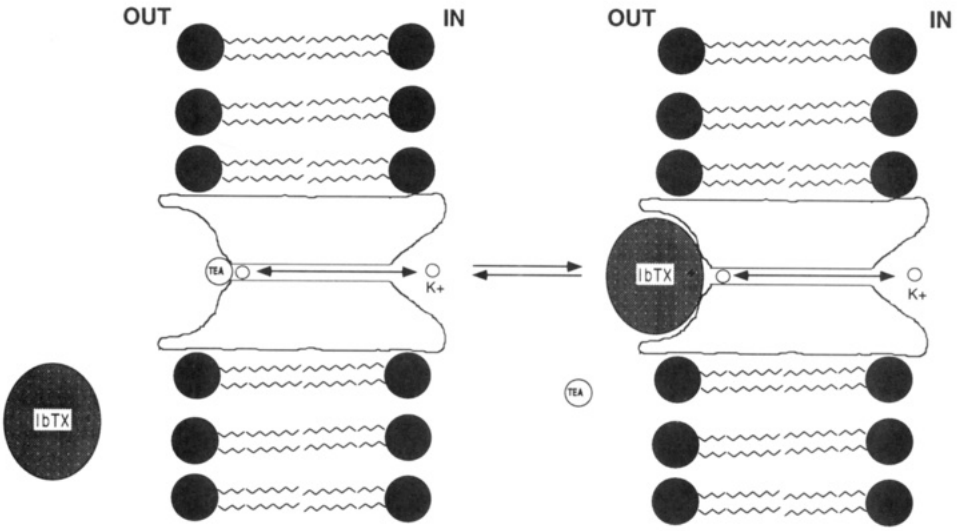

FIGURE 9: Model for IbTX block of the maxi-K channel. An ion channel in a membrane contains a central pore. IbTX binds to a site in the external mouth of the pore. TEA binds to a site in the external mouth that overlaps with the IbTX binding site. Potassium binds to a site in the pore near the external side and destabilizes IbTX bound to the channel.

The effect of external potassium on the association rate constant for IbTX could not be described by strict competition with a single potassium binding site on the channel, and external sodium produced qualitatively similar results. Taken together, these results suggest that the association of IbTX with the maxi-K channel is enhanced by a Coulombic attraction between the positively charged toxin and the negatively charged channel mouth.

Comparison with Charybdotoxin. The mechanism we propose for IbTX block of the maxi-K channel from smooth muscle is the same as the mechanism identified for ChTX block of the maxi-K channel from skeletal muscle (Anderson et al., 1988; MacKinnon & Miller, 1988; Miller, 1988; MacKinnon et al., 1989). The key features of ChTX block, including a 1:1 stochiometry for toxin block of the channel, trans-enhanced dissociation of toxin by internal potassium ions, and the role of surface electrostatics in toxin association with the channel, are also observed with IbTX. Both toxins appear to bind to a site near the external mouth of the pore and thereby occlude ion flux through the channel. Indeed, since both ChTX block (Miller, 1988) and IbTX block of the maxi-K channel in planar lipid bilayers exhibit strictly competitive behavior with TEA, it is likely that both toxins occupy similar binding domains on the maxi-K channel. These results appear to contradict previous findings where binding of ^{125}I-radiolabeled ChTX in bovine aortic sarcolemmal membranes did not exhibit strictly competitive behavior with unlabeled IbTX (Galvez et al., 1990). One explanation for this discrepancy is that iodination of ChTX modifies its interaction with the channel so that the binding sites for ^{125}I-ChTX and IbTX no longer overlap.

In retrospect, it is not surprising that ChTX and IbTX share similar binding domains on the maxi-K channel since the two toxins share 68% sequence homology (Gimenez-Gallego et al., 1988; Galvez et al., 1990) and similar three-dimensional structures (Bontems et al., 1991a; Johnson & Sugg, 1992). Six positively charged residues are conserved between the toxins, and five of these are localized to one part of the molecule. The structural similarity in this part of the toxins might underlie the functional similarities observed for the toxins.

Although IbTX and ChTX appear to share a common mechanism for block of maxi-K channels, we note some quantitative differences in the blocking kinetics. The most striking difference between IbTX and ChTX is the duration of the dwell times of the toxins on the channel. In symmetric 150 mM KCl and +40 mV, ChTX produces mean blocked times of about 64 s for maxi-K channels from bovine aortic smooth muscle (unpublished observations), while IbTX produces mean blocked times of about 840 s. This 13-fold difference represents a 1.5 kcal/mol difference in the energy barrier associated with toxin dissociation, slightly less than the energy of a hydrogen bond.

The effects of internal potassium concentration on IbTX dissociation suggest that potassium binding to a site in the pore destabilizes the IbTX–channel interaction by 57-fold. This binding site displays an apparent dissociation constant of 110 mM when the channel is blocked by IbTX and the site equilibrates with internal potassium. These results differ quantitatively from those determined by MacKinnon and Miller (1988) for ChTX block of the maxi-K channel from skeletal muscle, where the K_{K^+} value for the potassium site was 390 mM and occupancy of the potassium site was predicted to maximally destabilize the ChTX–channel interaction 20-fold. One could attribute these discrepancies to differences in maxi-K channels derived from smooth and skeletal muscle. Alternatively, the differences in the apparent affinities at the potassium binding site with ChTX or IbTX present could arise from subtle differences in how the two toxins interact with the maxi-K channel. If occupancy of the potassium binding site interacts with and destabilizes the toxin–channel interaction, it seems reasonable to assume that occupancy of the toxin binding site interacts with and alters the affinity of potassium for its site. Thus, the reported K_{K^+} values for the potassium binding sites are apparent and may be differentially influenced by features of the toxin–channel interaction which are unique to IbTX and ChTX.

The second-order association rate for IbTX of 1.3×10^6 M^{-1} s^{-1} in 150 mM KCl is about 4-fold slower than that observed for ChTX (unpublished observations). The association rate for IbTX decreased by 25-fold as the external potassium concentration was raised by 12-fold from 25 to 300 mM. In contrast, the association rate of ChTX binding to the maxi-K channel from skeletal muscle decreases by about 100-fold over this range of potassium concentrations (Anderson et al., 1988). Taken together, these results suggest that at low ionic strength, the differences in the observed collisional interactions for ChTX and IbTX result from differences in

electrostatic interactions between the toxins and the channel. While at high ionic strength, the slower k_{on} value for IbTX relative to ChTX results from other factors.

The structural differences between IbTX and ChTX should underlie the kinetic differences between the toxins. ChTX is a highly basic molecule with a net charge of +5 at neutral pH, while IbTX carries a net charge of +1. Both toxins contain seven positively charged residues. The difference in net charge results from four additional negatively charged aspartic acid residues on IbTX. The differences in the charge profiles for ChTX and IbTX provide a natural explanation for some of the differences in their association rate constants. The smaller net charge on IbTX could lead to a reduced Coulombic attraction between the toxin and the channel, and thus explain the smaller effect of ionic strength on the IbTX association rate relative to ChTX. This is consistent with the finding that the charge product derived from Debye–Huckel theory for the IbTX–channel interaction was −3.7 while the fit of this theory to the data of Anderson et al. (1988) yielded a charge product of −5.5 for ChTX. While these findings are consistent with the smaller net charge of IbTX, the charge product for IbTX is greater than might be expected from its net charge of +1. Although these charge products are not quantitatively interpretable in the absence of structural data for both toxin and channel, they suggest that the Coulombic attraction between IbTX and the channel may be dominated by short-range interactions as has been observed for protein–protein interactions in other systems (Stonhuerner et al., 1979; Salemme, 1976).

The introduction of four aspartates into IbTX may also explain the slower k_{on} value obtained at high ionic strength, in the absence of significant long-range electrostatic interactions. IbTX contains a larger total number of charged residues than ChTX; 13 for IbTX, 9 for ChTX. If any of these extra charges interact with the channel, then desolvation of these residues might contribute to the slower association rate for IbTX at high ionic strength, where electrostatic interactions are attenuated.

We have shown that the mechanism for IbTX block of the maxi-K channel qualitatively resembles the mechanism for ChTX block as described by MacKinnon and Miller (1988), and Anderson et al. (1988). Further, since IbTX and ChTX both compete with TEA, we suggest that IbTX and ChTX occupy the same site near the mouth of the channel.

ACKNOWLEDGMENT

We thank Jeff Smith for advice on bilayer techniques, Ilya Feygin for building electronic equipment, Gregg King for constructing experimental equipment, and Ramon Latorre, Bruce Johnson, and Bill Ferguson for comments on the manuscript.

REFERENCES

Anderson, C. S., MacKinnon, R., Smith, C., & Miller, C. (1988) *J. Gen. Physiol. 91*, 317–333.
Barrett, J. N., Magleby, K. L., & Palotta, B. S. (1982) *J. Physiol. 331*, 211–230.
Bezanilla, F., & Armstrong, C. M. (1972) *J. Gen. Physiol. 60*, 588–608.
Blatz, A. L., & Magleby, K. L. (1984) *J. Gen. Physiol. 84*, 1–23.
Bontems, F., Roumestand, C., Boyot, P., Gilquin, B., Doljansky, Y., Menez, A., & Toma, F. (1991a) *Eur. J. Biochem. 196*, 19–28.
Bontems, F., Roumestand, C., Gilquin, B., Menez, A., & Toma, F. (1991b) *Science 254*, 1521–1523.
Bronsted, J. N. (1922) *Z. Phys. Chem. 102*, 169–207.
Candia, S., Garcia, M. L., & Latorre, R. (1991) *Biophys. J. 59*, 213a.
Galvez, A., Gimenez-Gallego, G., Reuben, J. P., Roy-Contancin, L., Feigenbaum, P., Kaczorowski, G. J., & Garcia, M. L. (1990) *J. Biol. Chem. 265*, 11083–11090.
Giangiacomo, K. M., Garcia, M. L., & McManus, O. B. (1991) *Biophys. J. 59*, 79a.
Gimenez-Gallego, G., Navia, M. A., Reuben, J. P., Katz, G. M., Kaczorowski, G. J., & Garcia, M. L. (1988) *Proc. Natl. Acad. Sci. U.S.A. 85*, 3329–3333.
Green, W. N., Weiss, L. B., & Andersen, O. S. (1987) *J. Gen. Physiol. 89*, 873–903.
Johnson, B. A., & Sugg, E. E. (1992) *Biochemistry* (in press).
Lambert, P., Kuroda, H., Chino, N., Watanabe, T. X., Kimura, T., & Sakakibara, S. (1990) *Biochem. Biophys. Res. Commun. 170*, 684–690.
MacKinnon, R., & Miller, C. (1988) *J. Gen. Physiol. 91*, 335–349.
MacKinnon, R., & Miller, C. (1989) *Biochemistry 28*, 8087–8092.
MacKinnon, R., Latorre, R., & Miller, C. (1989) *Biochemistry 28*, 8092–8099.
McManus, O. B., Blatz, A. L., & Magleby, K. L. (1987) *Pfluegers Arch. 410*, 530–553.
Miller, C. (1988) *Neuron 1*, 1003–1006.
Miller, C., Moczydlowski, E., Latorre, R., & Phillips, M. (1985) *Nature 313*, 316–318.
Ravindran, A., & Moczydlowski, E. (1989) *Biophys. J. 55*, 359–365.
Salemme, F. R. (1976) *J. Mol. Biol. 102*, 563–568.
Slaughter, R. S., Shevell, J. L., Felix, J. P., Garcia, M. L., & Kaczorowski, G. J. (1989) *Biochemistry 28*, 3995–4002.
Stonehuerner, J., Williams, J. B., & Millett, F. (1979) *Biochemistry 18*, 5422–5427.
Sugg, E. E., Garcia, M. L., Reuben, J. P., Patchett, A. A., & Kaczorowski, G. J. (1990) *J. Biol. Chem. 265*, 18745–18748.
Villaroel, A., Alvarez, O., Oberhauser, A., & Latorre, R. (1988) *Pfluegers Arch. 413*, 118–126.
Wherland, S., & Gray, H. B. (1976) *Proc. Natl. Acad. Sci. U.S.A. 73*, 2950–2954.
Yellen, G. (1984) *J. Gen. Physiol. 84*, 157–186.

Registry No. IbTX, 129203-60-7.